

X4

Copy 228  
RM L50L20

NACA RM L50L20

7230

TECH LIBRARY KAFB, NM  
0143762

NACA

# RESEARCH MEMORANDUM

EFFECTS OF SPOILER ON AIRFOIL PRESSURE DISTRIBUTION AND  
EFFECTS OF SIZE AND LOCATION OF SPOILERS ON THE  
AERODYNAMIC CHARACTERISTICS OF A TAPERED  
UNSWEPT WING OF ASPECT RATIO 2.5

AT A MACH NUMBER OF 1.90

By D. William Conner and Meade H. Mitchell, Jr.

Langley Aeronautical Laboratory  
Langley Field, Va.

CLASSIFIED DOCUMENT

Information affecting the National Defense of the United States within the meaning of the Espionage Laws, Title 18, United States Code, is hereby declared to be classified and its transmission or the revelation of its contents in any manner to an unauthorized person is prohibited by law. Information so classified may be imparted only to personnel of the United States, appropriate civilian officers and employees of the Federal Government, and to United States citizens of known loyalty and discretion who of necessity must be so informed.

NATIONAL ADVISORY COMMITTEE  
FOR AERONAUTICS

WASHINGTON  
January 24, 1951

314.98/13

Classification: UNCLASSIFIED

By Author:

NASA Tech Pub Announcement #11

By

28 Jun 67

GRADE OF OFFICER MAKING CHANGE)

4 Apr 68

DATE



0143762

1  
NACA RM L50L20

## NATIONAL ADVISORY COMMITTEE FOR AERONAUTICS

## RESEARCH MEMORANDUM

EFFECTS OF SPOILER ON AIRFOIL PRESSURE DISTRIBUTION AND

EFFECTS OF SIZE AND LOCATION OF SPOILERS ON THE

AERODYNAMIC CHARACTERISTICS OF A TAPERED

UNSWEPT WING OF ASPECT RATIO 2.5

AT A MACH NUMBER OF 1.90

By D. William Conner and Meade H. Mitchell, Jr.

## SUMMARY

An investigation has been made in the Langley 9- by 12-inch supersonic blowdown tunnel of spoilers on two unswept wing arrangements at Mach numbers of 1.90 and 1.96 and Reynolds numbers of  $2.2 \times 10^6$  and  $1.3 \times 10^6$ , respectively.

The results of pressure-distribution tests on an unswept airfoil in the presence of a fuselage but without tip effects indicated that spoilers could be oppositely deflected in a manner similar to flap-type ailerons to obtain roll effectiveness without loss in lift. When the angle of attack was increased from  $0^\circ$  to  $10^\circ$ , the effectiveness of a spoiler projected 0.05 wing chord above the upper surface showed a slight decrease, whereas the effectiveness of the same spoiler projected from the lower surface was almost double the effectiveness of the upper-surface spoiler.

The rolling effectiveness of spoilers deflected from the upper surface of a semispan wing of aspect ratio 2.5 was usually increased as the spoiler location was moved toward the wing trailing edge and was little affected by inboard movement. Spoiler drag decreased rapidly as the angle of attack was increased. The data indicated that, for controls located near the wing trailing edge and providing the same amount of roll control, spoiler drag approached flap-type-aileron drag at an angle of attack of about  $6^\circ$ .

## INTRODUCTION

In the transonic and supersonic speed range, spoiler-type controls can offer desirable qualities not always found in flaps, such as high control effectiveness at transonic speeds, low control forces, and low wing-twisting moments. The maximum control effectiveness that can be obtained with a spoiler may be limited, however, since it is difficult to obtain large projections of the spoiler and still allow the spoiler to be accommodated inside the wing in the retracted position. Adequate theory is not yet available to even indicate trends of spoiler characteristics, and therefore experimental studies must be used to obtain such information. To supplement the rather limited exploratory work already done on spoilers at these speeds (see references 1 and 2), spoilers have been included for investigation in a program being carried out in the Langley 9- by 12-inch supersonic blowdown tunnel to study some of the effects of design parameters on control characteristics. To study in detail the effects of spoiler projection on chordwise loading, pressure-distribution measurements were obtained on an unswept airfoil in the presence of a fuselage but without tip effects. These data are presented herein for a Mach number of 1.96. The experimental force and moment data obtained at a Mach number of 1.90 of spoilers tested in conjunction with an unswept semispan wing of aspect ratio 2.5 are also presented. A similar investigation of plain flap-type controls has already been carried out with the same wing (reference 3).

The airfoil containing pressure orifices had 10-percent-thick hexagonal airfoil sections. Chordwise- and spanwise-pressure-distribution measurements were obtained over the airfoil in a region extending out from a fuselage mounted in the center of the test section. Tests were conducted through an angle-of-attack range of  $-10^\circ$  to  $10^\circ$  at a Reynolds number of  $1.3 \times 10^6$  with and without a spoiler projected 5 percent of the airfoil chord and located at the 62-percent-chord station.

The wing of aspect ratio 2.5 was unswept and had a taper ratio of 0.625 and 6-percent-thick hexagonal airfoil sections. Spoiler configurations included spans that varied from 25 to 75 percent of the wing semispan and chordwise locations that varied from 55 to 75 percent of the wing chord. Spoilers were projected from 0 to 5 percent of the local chord. The investigation was carried out at a Reynolds number of  $2.2 \times 10^6$  through angles of attack ranging from  $-4^\circ$  to  $3^\circ$ . All tests were made with the wing in the presence of a fuselage. Five-component-force and moment data were obtained, and the results are compared with those of the wing-flap tests reported in reference 3.

## COEFFICIENTS AND SYMBOLS

All data are presented with respect to the wind axes.

$C_L$	lift coefficient $\left( \frac{\text{Lift}}{qS} \right)$
$C_D$	drag coefficient $\left( \frac{\text{Drag}}{qS} \right)$
$C_m$	pitching-moment coefficient $\left( \frac{\text{Pitching moment about } 0.5\bar{c}}{qS\bar{c}} \right)$
$C_{l_{\text{gross}}}$	gross rolling-moment coefficient $\left( \frac{\text{Wing panel rolling moment}}{2qSb} \right)$
$C_{n_{\text{gross}}}$	gross yawing-moment coefficient $\left( \frac{\text{Wing panel yawing moment}}{2qSb} \right)$
$C_l$	rolling-moment coefficient $\left( C_{l_{\text{gross}}} - C_{l_{\text{gross}}(h=0)} \right)$
$C_n$	yawing-moment coefficient $\left( C_{n_{\text{gross}}} - C_{n_{\text{gross}}(h=0)} \right)$
$\Delta C_L, \Delta C_D, \Delta C_m$	increment in coefficient due to spoiler projection
$P$	pressure coefficient $\left( \frac{P_{\text{measured}} - P_{\text{static}}}{q} \right)$
$P_{\text{measured}}$	orifice pressure
$P_{\text{static}}$	test section static pressure as determined from measurements of stagnation pressure and average test section Mach number
$q$	free-stream dynamic pressure
$S$	exposed semispan-wing area (10.00 sq in.)

$\bar{c}$	mean aerodynamic chord of exposed wing area (3.13 in.)
$c$	local wing chord
$b$	twice the distance from the wing root to the wing tip (8.13 in.)
$b_s$	spoiler span
$y$	spanwise distance from fuselage, inches
$x$	chordwise distance from airfoil leading edge
$y_s$	spanwise location of inboard end of spoiler
$h$	spoiler projection normal to the wing-chord plane
$\delta$	flap deflection normal to flap hinge line
$\alpha$	angle of attack relative to free-stream direction
$R$	Reynolds number based on $\bar{c}$
$M$	Mach number

## MODEL

The unswept airfoil which contained pressure orifices is shown in figure 1 and was fabricated of tool steel and was so arranged as to permit spanwise movement with a close sliding fit through the strut-mounted body. The 38-percent-chord wedge-shaped leading and trailing edges had included wedge angles of about  $15^\circ$ . The center 24 percent of the chord had a constant 10-percent-chord thickness. The brass spoiler which was screwed to the airfoil was 0.05c thick and its leading edge was located at the 62-percent-chord station. The top edge was beveled to a knife edge as shown in figure 1 to approximate the airfoil loading conditions produced by a thin spoiler projected 5 percent of the airfoil chord. With spoiler removed, both the screw holes in the airfoil and the notch in the body were filled with cold-process metal solder.

A photograph of the semispan wing and the half-fuselage installed in the tunnel test section is presented in figure 2. The geometry of the configuration is detailed in figure 3. The body had the same nose contour but was 1.25 the scale of the body used in the pressure tests. The steel wing, which was also used in the flap-effectiveness tests of

reference 3, was unswept at the midchord line and had a taper ratio of 0.625 and an aspect ratio of 2.5 based on the wing area which included that part of the wing enclosed by the fuselage. The 30-percent-chord wedge-shaped leading and trailing edges had included wedge angles of  $11.43^\circ$  measured streamwise. The center 40 percent of the chord had a constant 6-percent-chord thickness. The spoiler-type controls were constructed from 0.030-inch sheet brass and soldered in small machined grooves in the wing normal to the chord plane (see fig. 3). The top edges of the spoilers were then filed down to attain successive projections of 5, 2, and 1 percent of the local wing chord. Spoilers of three different spans were tested at each of three chordwise locations. Spans and spanwise locations included two 0.25b/2 spoilers with the inboard end located at 0.70b/2 and at 0.45b/2, a 0.50b/2 spoiler with the inboard end located at 0.45b/2, and a 0.75b/2 spoiler with the inboard end located at 0.20b/2 (adjacent to the body). Chordwise locations included the 55-, 65-, and 75-percent-chord stations.

#### TUNNEL AND TEST TECHNIQUE

The present tests were conducted in the Langley 9- by 12-inch supersonic blowdown tunnel which is of the nonreturn type and which utilizes the exhaust air of the Langley 19-foot pressure tunnel. The absolute pressure of the inlet air is approximately  $2\frac{1}{3}$  atmospheres.

Subsequent to the initial phase of the program in which the force and moment tests were carried out at  $M = 1.90$ , heating and drying equipment was installed to produce condensation-free flow. The Mach number was increased to 1.96, and the pressure-distribution tests were then made with the air conditioned to a dew point of  $-20^\circ\text{F}$  or below and heated to a stagnation temperature of  $170^\circ\text{F}$  or above.

For the pressure-distribution tests the dynamic pressure and test Reynolds number decreased about 8 percent during the course of each run because of the decreasing pressure of the inlet air. The average dynamic pressure was 11 pounds per square inch, and the average Reynolds number was  $1.3 \times 10^6$ . For the force tests the dynamic pressure and test Reynolds number decreased about 3.5 percent during the course of each run. The average dynamic pressure was 11.5 pounds per square inch, and the average Reynolds number was  $2.2 \times 10^6$ . In making pressure-distribution tests, the body was strut-mounted in the center of the test section and the untapered, unswept airfoil was extended through it from one wall of the tunnel. The airfoil was of considerable length and was so arranged as to be moved spanwise through the body. A band of pressure orifices was located on the airfoil and, by spanwise movement of the airfoil, the pressure distribution over the

airfoil was measured (without tip effects) from the body outboard to the region where wall-reflected disturbances existed.

The semispan-wing model was attached in a cantilever arrangement through a half-fuselage to a strain-gage balance. The balance mounts flush with the tunnel wall and rotates with the model through the angle-of-attack range. To minimize the boundary-layer effects, the fuselage was shimmed out 0.25 inch from the tunnel wall and mounted on the balance housing; thus the wing could be tested in the presence of, but not attached to, the fuselage. Because of balance deflections under load, a gap of approximately 0.015 inch was maintained between the wing and fuselage under the no-load condition. The gap size limited the angle-of-attack range from  $-4^{\circ}$  to  $8^{\circ}$ . Further discussion of the test-technique development and of possible factors which might influence the test results is given in references 3 and 4.

#### ACCURACY

Free-stream Mach number has been calibrated at 1.90 and 1.96 with variation of  $\pm 0.02$  for the two test arrangements. Calibration with the tunnel clear indicated that the static pressure varied  $\pm 1.5$  percent in the test section region and the stream angle varied  $\pm 0.25^{\circ}$ .

No tare corrections have been applied to any of the data presented. In some instances small errors in fabrication and model setup caused asymmetrical conditions as indicated (for example, in the pitching-moment data of fig. 8). These slightly asymmetrical conditions would not, however, affect the value of the data for comparative purposes. The magnitude of the random errors that existed, based on the accuracy of the measuring and recording equipment and fluctuations of the air stream, are believed to be of the following order:

<u>Variable</u>	<u>Error</u>
$\alpha$ , degrees . . . . .	$\pm 0.05$
$C_l$ . . . . .	$\pm 0.001$
$C_L$ . . . . .	$\pm 0.005$
$C_D$ . . . . .	$\pm 0.001$
$C_m$ . . . . .	$\pm 0.002$
$C_n$ . . . . .	$\pm 0.0002$
P . . . . .	$\pm 0.003$

In filing the spoilers to obtain the desired heights, the projection (h) at all spanwise stations was held within  $\pm 0.001$  chord. Measuring accuracy was in the order of  $\pm 0.0005$  chord, and therefore the absolute values of h at any station are accurate within limits of  $\pm 0.0015$  chord.



## RESULTS AND DISCUSSION

## Pressure-Distribution Tests

Figure 4 presents the experimental pressure-distribution data obtained with and without a spoiler located on the airfoil. These curves are based on experimental points obtained at intervals in the y-direction of 0.1 inch immediately adjacent to the body and 0.25 inch at the outermost stations. In order to indicate clearly small differences between curves, symbols have not been used since many experimental points fall on or very close to one another. These data have been cross plotted in figure 5 to show the chordwise loading on the airfoil at three spanwise stations out from the body. Because of the limited number of chordwise orifice stations, the experimental curves have arbitrarily been faired to have sudden changes in pressure at the airfoil-surface break lines in the same manner as the theoretical pressure distribution of the airfoil without spoiler in two-dimensional flow (also presented in fig. 5).

The results of figure 5 indicate that projecting the spoiler section out of the wing upper surface did not change the pressure distribution on the lower surface except for orifice number 5 at zero angle of attack where the pressure was changed a slight amount. The reason for this change was not clear, although it may have resulted from an unclean condition of the airfoil. On the upper surface the pressure distribution was affected in about the same manner as if wedge-shaped thickness were added to that surface such that the thickness increased with increase in the chordwise ordinate until a ridge line was reached which coincided with the top of the spoiler. Negative increments of normal force occurred ahead of the spoiler in a region of flow compression; positive increments occurred behind the spoiler in an expansion region. For all angles of attack the region of influence of the spoiler extended ahead onto the leading-edge wedge to a location lying between the first orifice (at 10 percent of the wing chord) and the second orifice (at 30 percent of the chord). Ahead of the spoiler the magnitude of the pressure increment decreased as the angle of attack was increased. This decrease is in accordance with shock theory which indicates that the pressure increment caused by turning the flow through a constant angle from some reference surface decreases in magnitude as the reference surface is inclined away from the air stream. Usually the negative pressure increment (positive normal force) behind the spoiler also decreased with increasing angle of attack. The magnitude of the positive normal-force increment to the rear of the spoiler was not large, and the net increment in lift loading caused by the spoiler remained negative and decreased in magnitude as the angle of attack was increased, especially from  $\alpha = -10^\circ$  to  $0^\circ$ . Since the

airfoil was symmetrical, the designation of the reference surfaces and signs of angle of attack can arbitrarily be reversed to permit consideration of the condition where the spoiler is projected from the lower surface of the airfoil. For such a condition the spoiler effectiveness increased with increasing angle of attack and, at  $10^\circ$ , was almost double the effectiveness of the upper-surface spoiler. These results indicate that roll control with little or no change in lift could be obtained in the same manner as with flap-type ailerons on a complete wing by simultaneous control deflection (in opposite directions) of the two spoilers.

Projection of the spoiler at this chordwise location would cause a nose-down pitching moment about the airfoil midchord point, mainly as a result of the lift change behind the spoiler rather than ahead of the spoiler since the center of the negative-lift load ahead of the spoiler about coincided with the pitch axis.

Somewhat smaller increments in loading were measured at 0.1 inch from the body than were measured farther out, but there were no large effects of spanwise location on the chordwise distribution of the added loading attributed to the spoiler.

#### Force and Moment Tests

Basic test data for the aspect-ratio-2.5 wing are presented in figures 6 to 10 where the aerodynamic coefficients are plotted against angle of attack. These plots are for the wing with spoilers located at the 75-percent-chord station only and are representative of all the experimental data. Corresponding basic-data plots for spoilers located at the 65- and 55-percent-chord station are therefore omitted. Cross plots of the data for the various spoiler spans, spanwise locations, and chordwise locations are presented in figures 11 to 15 where the increments of the coefficients are plotted against spoiler projection for several angles of attack. Symbols were used in the plots to show clearly the trends in the aerodynamic coefficients and the incremental values taken from the unrepresented data.

Effect of angle of attack.- The semispan-wing tests were carried out prior to the pressure-distribution measurements, and, unfortunately, the angle-of-attack range selected did not include the more negative angles where information concerning the effects of spoilers on the high-pressure side of the wing would have been obtained. For the angle-of-attack range from  $-3^\circ$  to  $6^\circ$  the magnitude of the rolling moment (fig. 11) and lift effectiveness (fig. 12) changed only slightly. This effect is in contrast with the pressure-distribution data of figure 5, where the normal-force incremental loading tended to decrease with increasingly positive angle of attack. No definite variation of the incremental pitching moment occurred with changing angle of attack (fig. 13) except

for the  $0.75\frac{b}{2}$ -span spoilers projected  $0.05c$  and located at the  $0.65$ - and  $0.55$ -chord station. For these configurations the negative increments decreased in magnitude with increasing angle of attack. There was a reduction of about one-half in the value of the incremental drag coefficient (fig. 14) and negative yawing-moment coefficient (fig. 15) as the angle of attack was increased from  $-3^\circ$  to  $6^\circ$ . About two-thirds of the incremental-drag reduction was due to decreasing chord force, whereas one-third resulted from the change in inclination of the nearly constant negative normal-force component. The change in yawing moment was due mainly to the incremental-drag change rather than to any shift in the spanwise center of pressure.

Effect of chordwise location on spoiler effectiveness.- The data of figure 11 indicate that rearward spoiler movement generally caused a small increase in rolling-moment effectiveness. A similar increase was noted in the free-flight rocket tests of spoilers on an unswept wing (reference 1). This increased rolling effectiveness was associated with an increase in the magnitude of the negative lift increment (fig. 12) which occurred when the spoilers were moved toward the trailing edge, probably because of decreasing positive lift behind the spoiler. The pitching-moment increments (fig. 13) generally became positive when the spoiler was moved rearward to the  $0.75c$  station. This positive change indicates a sizable rearward shift in the location of the effective center of the negative spoiler lift as would be expected for rearward spoiler movement. The magnitude of the spoiler drag (fig. 14) did not seem to be affected by chordwise location except for the full-span condition where the middle location (at  $0.65c$ ) caused the greatest drag rise at low and negative angles of attack. This high drag and the negligible pitching moment suggest that, for a midchord center-of-gravity location, the  $0.75\frac{b}{2}$ -span spoilers located at the  $0.65$ -chord station and deflected from the lower surface would be most suitable for use as speed brakes.

Effect of spoiler-span and spanwise location on spoiler effectiveness.- Maximum values of rolling moment (fig. 11) were measured for spoilers with spans equal to  $0.75\frac{b}{2}$ . These values varied almost linearly with spoiler projection throughout the range tested. As inboard sections were removed, however, losses occurred in rolling-moment effectiveness that resulted in nonlinear and even zero effectiveness characteristics for the lower spoiler projections, especially at the highest angles of attack. For spoilers projected  $0.05c$ , rolling-moment effectiveness was little influenced by changes in angle of attack regardless of span. When the  $0.25\frac{b}{2}$  spoiler was moved inboard from  $y_g$  equal to  $0.70\frac{b}{2}$  to  $0.45\frac{b}{2}$ , the rolling moment was not appreciably affected because the decrease in moment-arm length was usually offset by an increase in lift effectiveness. This increase in lift effectiveness was probably a result of a greater area affected by the spoiler at the inner location as well as freedom from the loading losses under the wing-tip Mach cone which existed for the outboard spoiler location. The lift and rolling-moment

effectiveness of the two  $0.25b/2$  spoilers projected simultaneously  $0.05c$  generally equaled the sum of their individual effectiveness values.

Comparison of spoiler and flap-type control.- The results of these tests have been compared with the flap tests on this wing (reference 3) on a basis of equal control spans and equal spanwise and chordwise locations of the spoilers and flap hinge lines. For a spoiler projection equal to  $0.05c$ , equivalent effectiveness values of  $C_l$  and  $\Delta C_L$  were measured at flap deflections of approximately  $3^\circ$ ,  $5^\circ$ , and  $8^\circ$  for chordwise locations of the spoiler and flap hinge line of  $0.55c$ ,  $0.65c$ , and  $0.75c$ , respectively.

A comparison has been made in figure 16 of the drag of the two types of controls for the condition of equal rolling-moment effectiveness ( $C_l = 0.007$ ) for controls extending from the body to  $0.95b/2$  and located at  $0.75c$ . As the angle of attack was increased, flap drag increased and spoiler drag decreased and the curves appear to converge at an angle of about  $6^\circ$ . It should be pointed out that the value of  $C_l$  of  $0.007$  would be about the maximum that could be expected from projecting a simple type of spoiler because the average required height of  $0.048c$  was about equal to the wing thickness at the spoiler location. Much higher maximum values of rolling moment than this value could be obtained with greater flap deflection, probably at the expense of high hinge moments. For this equal rolling-moment condition, the value of the pitching moment caused by spoiler projection was about one-fourth that caused by flap deflection. With opposite deflection of the controls at the same time on a complete wing, the spoiler would produce a slightly greater amount of adverse yawing moment and considerably more drag than would the flap for angles of attack up to  $6^\circ$ .

The results point out that, for certain conditions, spoilers compare favorably with flaps as control devices and merit further investigation, particularly at moderate and high angles of attack for oppositely deflected arrangements through a wide range of Mach numbers.

#### CONCLUDING REMARKS

A brief investigation has been made of spoilers in the Langley 9- by 12-inch supersonic blowdown tunnel. The results of pressure-distribution tests of an unswept airfoil at  $M = 1.96$  indicate that spoilers could be oppositely deflected in a manner similar to flap-type ailerons to obtain roll control without loss in lift. Projection of a spoiler from the airfoil surface affected the chordwise loading of an airfoil in much the same way as if wedge-shaped thickness were added to that surface such that the thickness increased with increase in chordwise ordinate until a ridge line was reached which coincided with the top of the spoiler.

When the angle of attack was increased from  $0^\circ$  to  $10^\circ$ , the effectiveness of the spoiler projected from the upper surface showed a slight decrease, whereas the effectiveness of the spoiler projected from the lower surface was almost double the effectiveness of the upper-surface spoiler. Spoiler effectiveness was not greatly influenced by the presence of a body.

The results of force and moment tests of an unswept semispan wing of aspect ratio 2.5 at  $M = 1.9$  indicate that the effectiveness of a spoiler deflected from the upper surface was usually increased as the spoiler location was moved toward the trailing edge and was little affected by inboard movement. Full-span spoilers had the most linear variation of effectiveness with projection. Spoiler drag, which was high at negative angles of attack, decreased rapidly as the angle of attack was increased. The data indicate that, for controls located near the wing trailing edge and providing the same amount of roll control, spoiler drag approached flap drag at an angle of attack of about  $6^\circ$ . With opposite deflection of the controls at the same time on a complete wing, the spoilers would have a slightly greater amount of adverse yawing moment than would flaps.

The results point out the need for further investigation of spoilers with regard to learning more about their characteristics at moderate and high angles of attack for oppositely deflected arrangements through a wide Mach number range.

Langley Aeronautical Laboratory  
National Advisory Committee for Aeronautics  
Langley Field, Va.

## REFERENCES

1. Strass, H. Kurt: Additional Free-Flight Tests of the Rolling Effectiveness of Several Wing-Spoiler Arrangements at High Subsonic, Transonic, and Supersonic Speeds. NACA RM L8I23, 1948.
2. Hammond, Alexander D.: Lateral-Control Investigation of Flap-Type and Spoiler-Type Controls on a Wing with Quarter-Chord-Line Sweepback of  $60^\circ$ , Aspect Ratio 2. Taper Ratio 0.6, and NACA 65A006 Airfoil Section. Transonic-Bump Method. NACA RM L50E09, 1950.
3. Mitchell, Meade H., Jr.: Effects of Varying the Size and Location of Trailing-Edge Flap-Type Controls on the Aerodynamic Characteristics of an Unswept Wing at a Mach Number of 1.9. NACA RM L50F08, 1950.
4. Conner, D. William: Aerodynamic Characteristics of Two All-Movable Wings Tested in the Presence of a Fuselage at a Mach Number of 1.9. NACA RM L8H04, 1948.

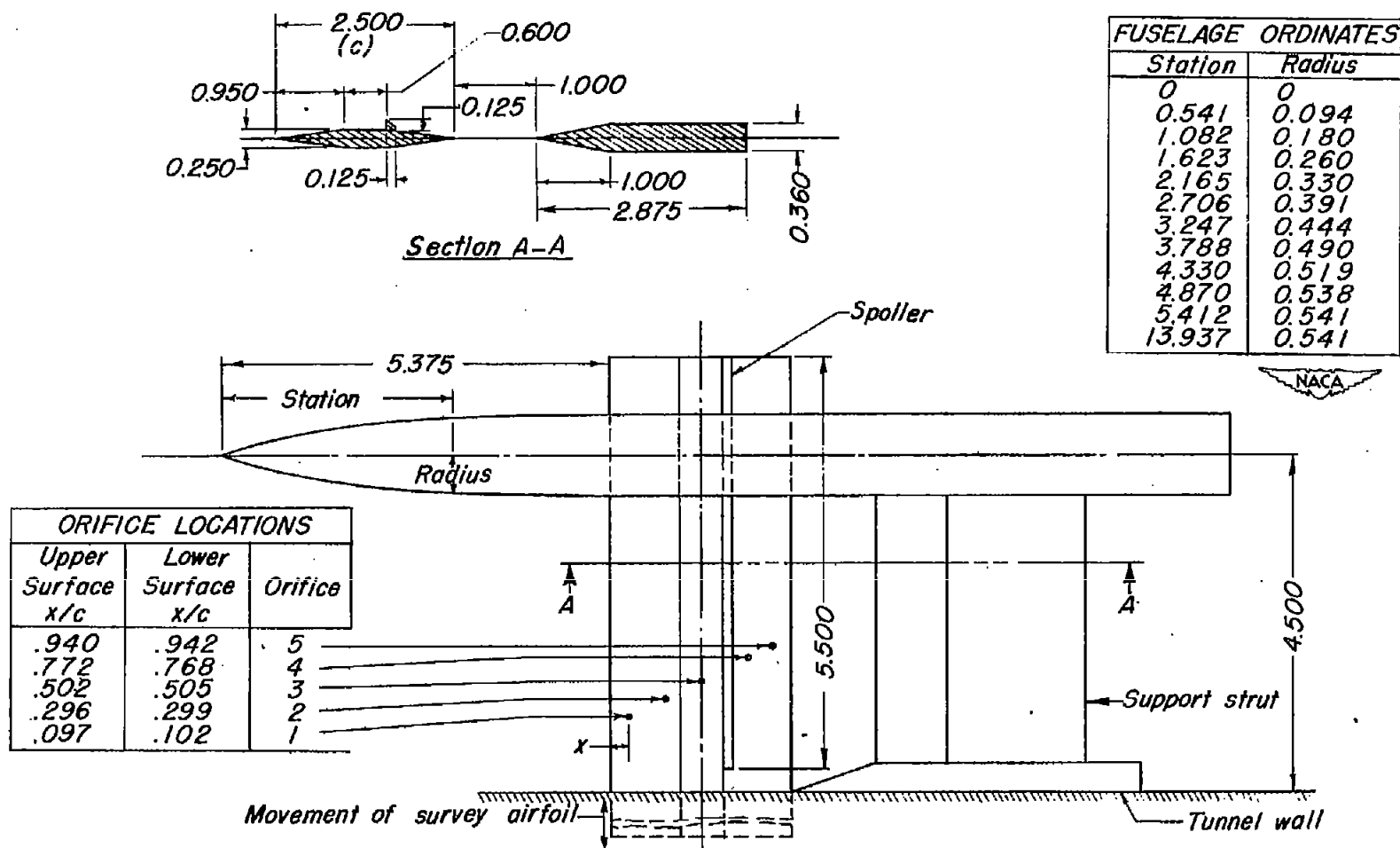


Figure 1:- Details of unswept airfoil and fuselage. All dimensions are in inches.





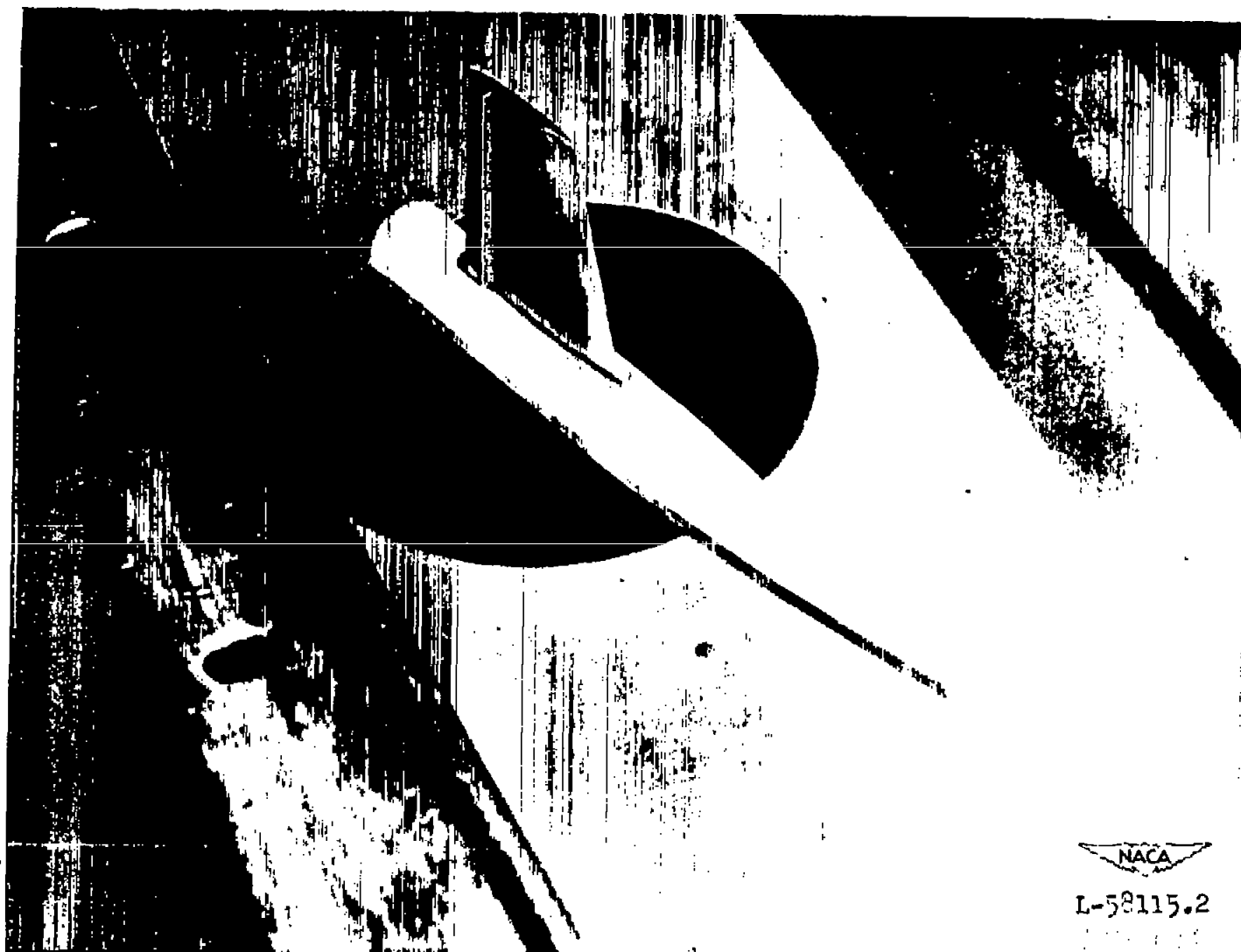


Figure 2.- Photograph of semispan model and spoiler-type control.



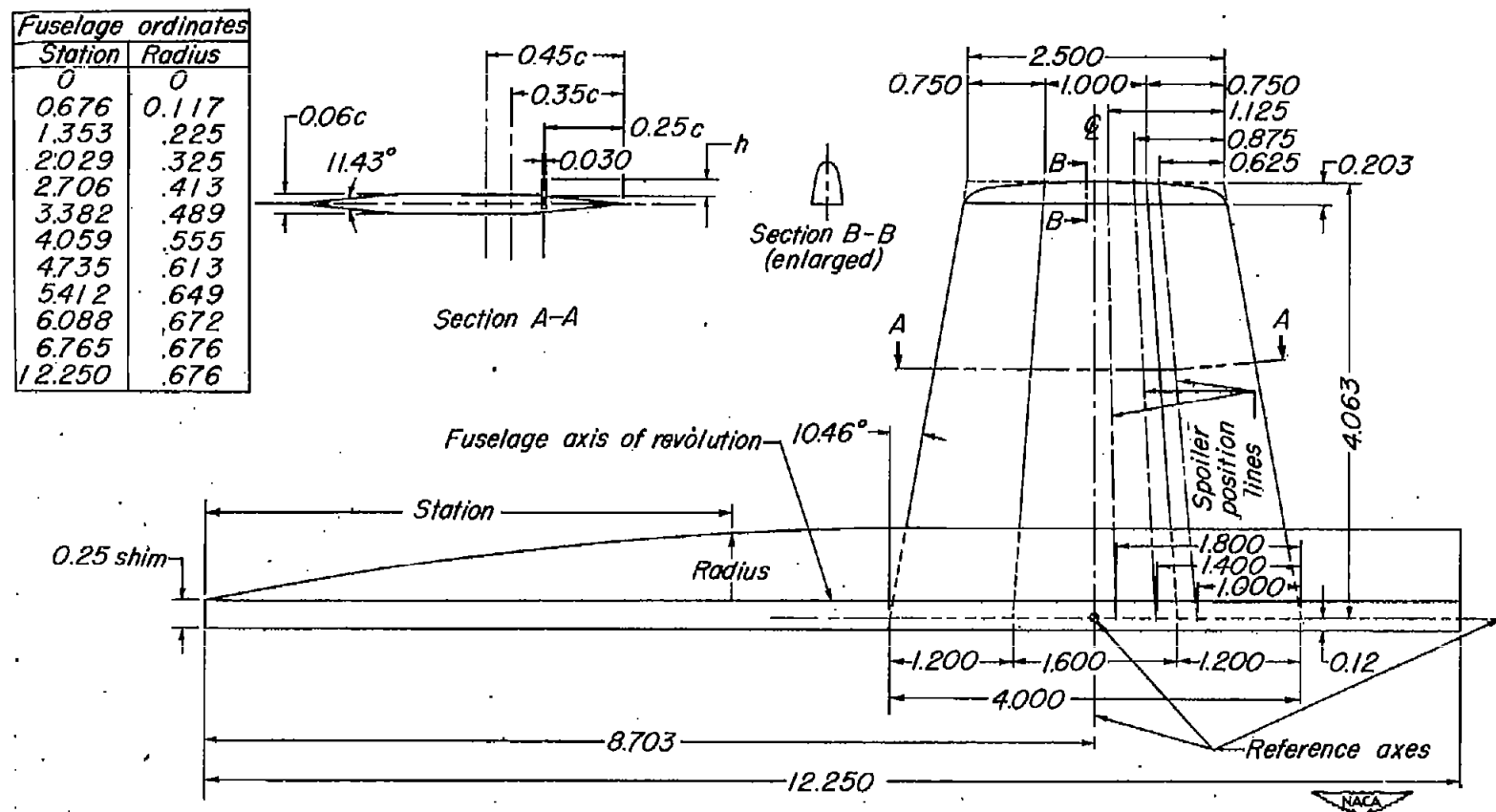


Figure 3.- Details of semispan wing model. All dimensions are in inches.

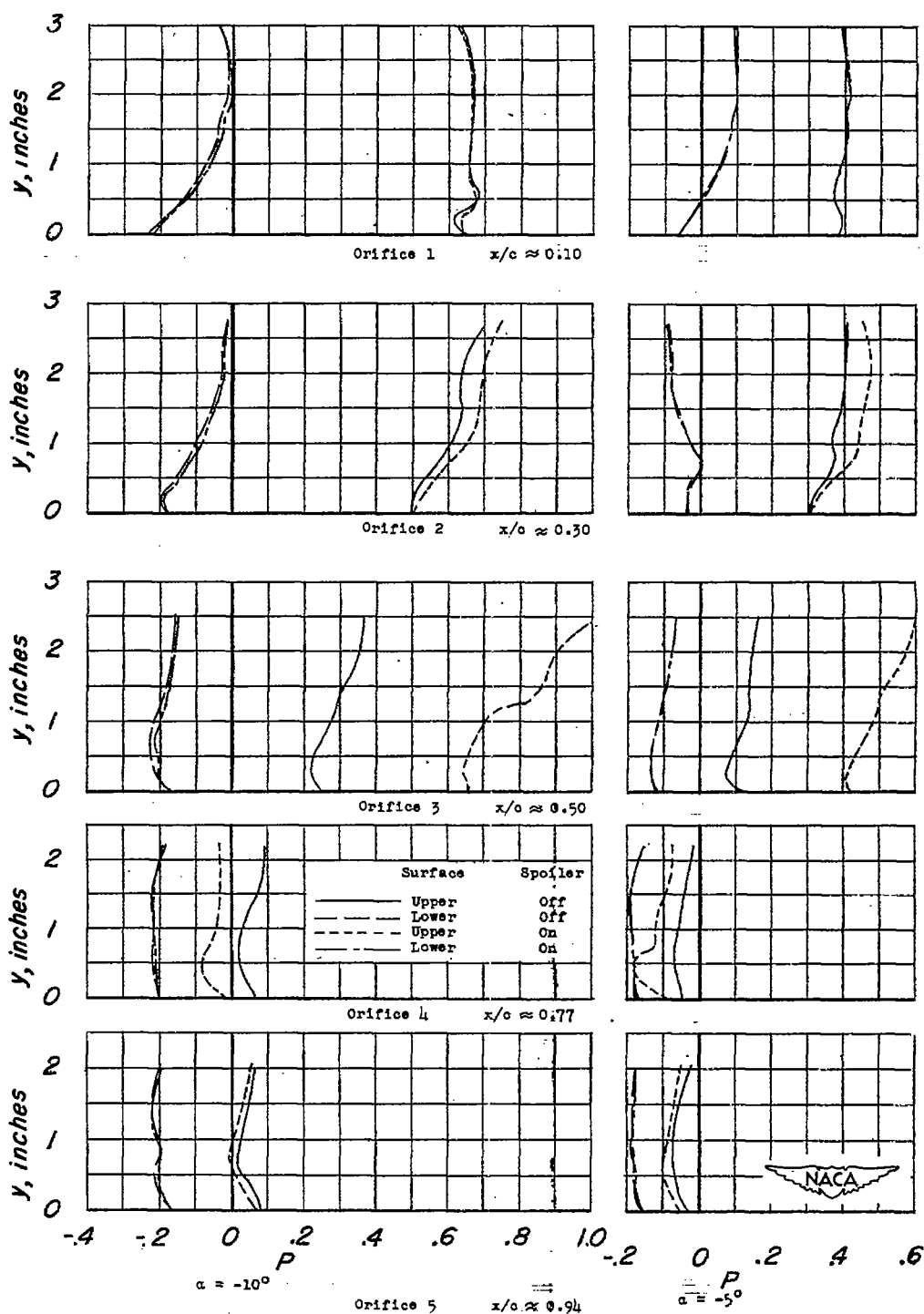


Figure 4.- Spanwise pressure distribution at each orifice for an unswept airfoil intersecting a fuselage with and without a spoiler projected 0.05c and located at  $\frac{x}{c} = 0.62$ .  $M = 1.96$ ;  $R = 1.3 \times 10^6$ .

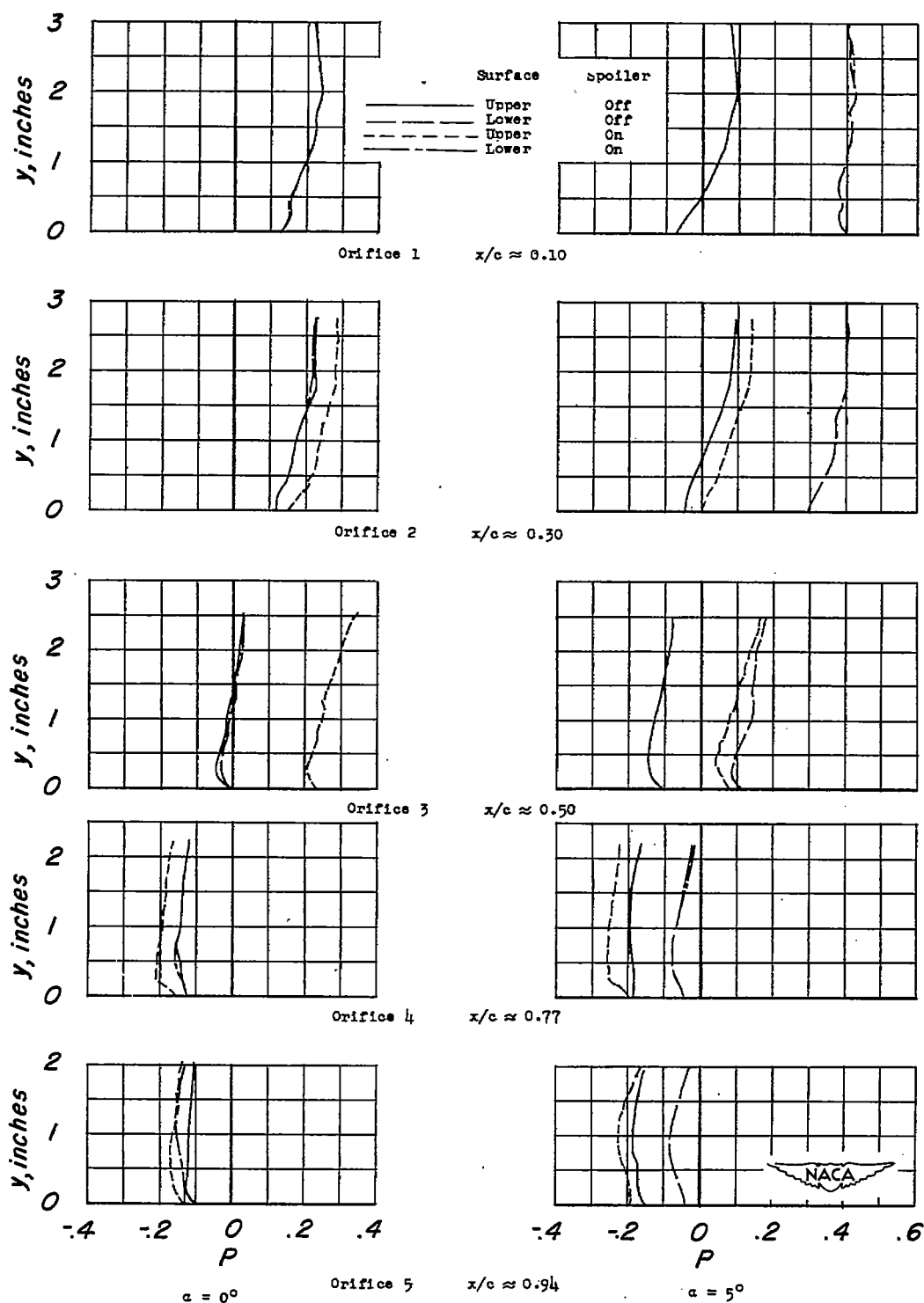


Figure 4.- Continued.

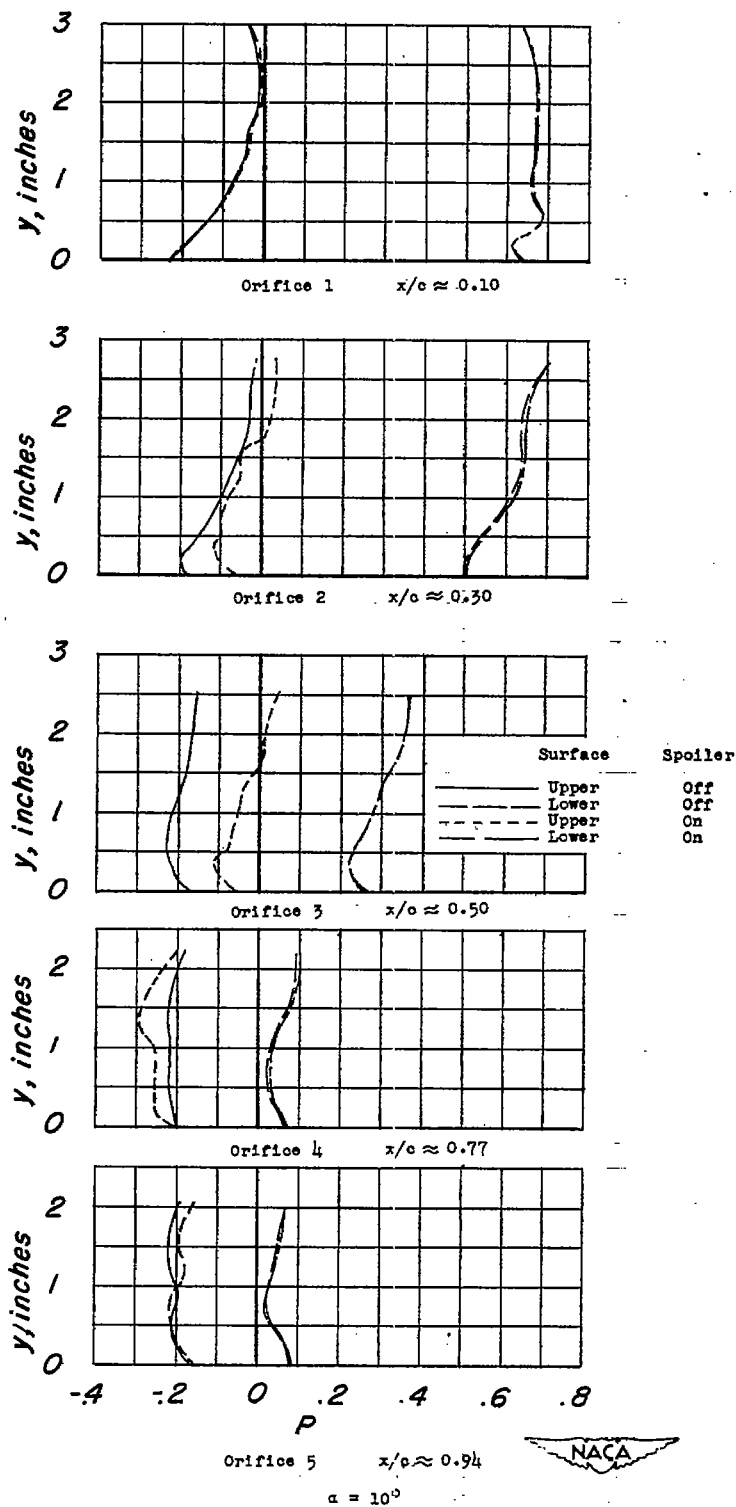
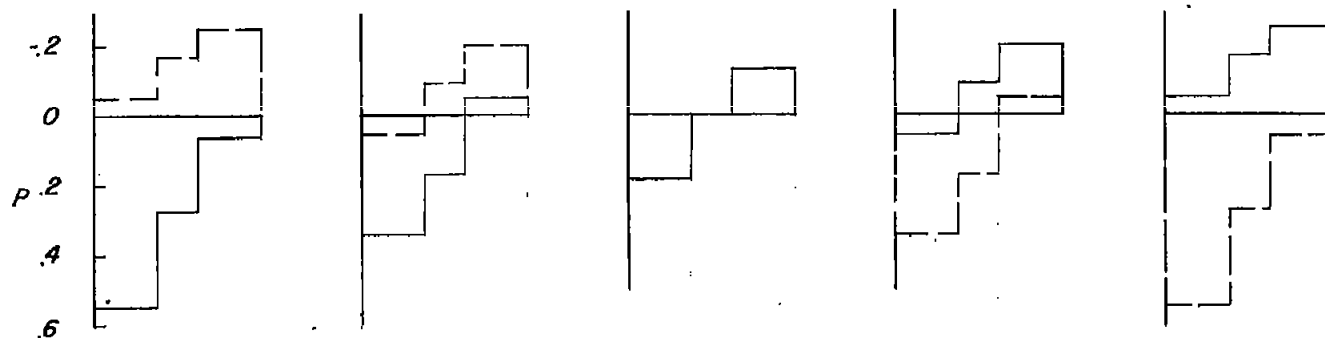


Figure 4.- Concluded.



(a) Calculated two-dimensional loading on airfoil without spoiler.

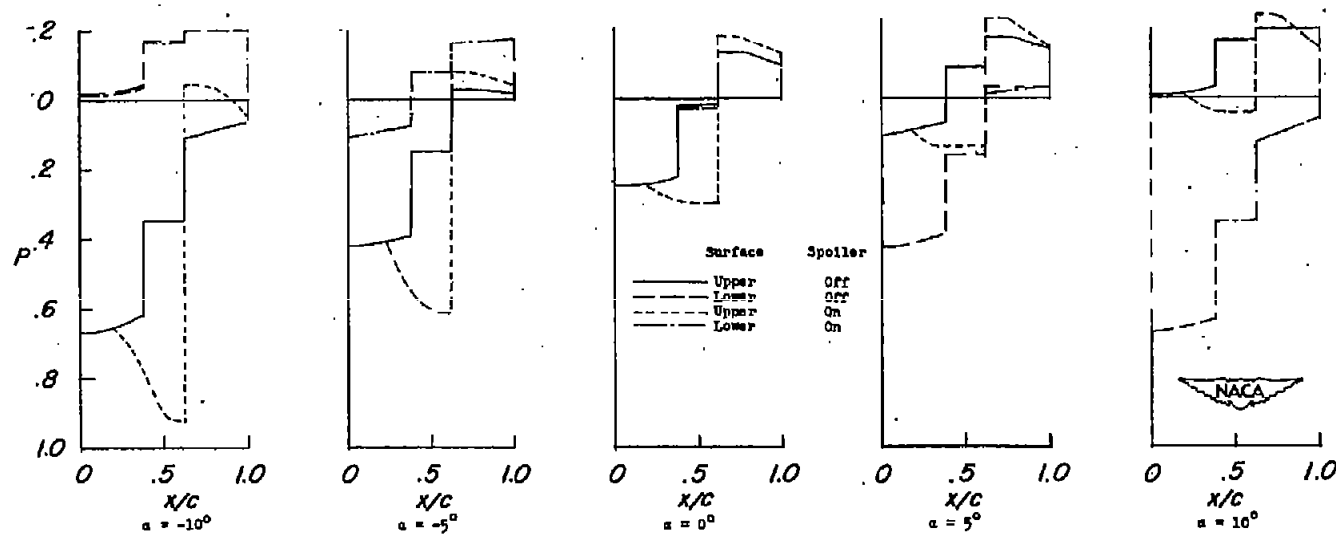
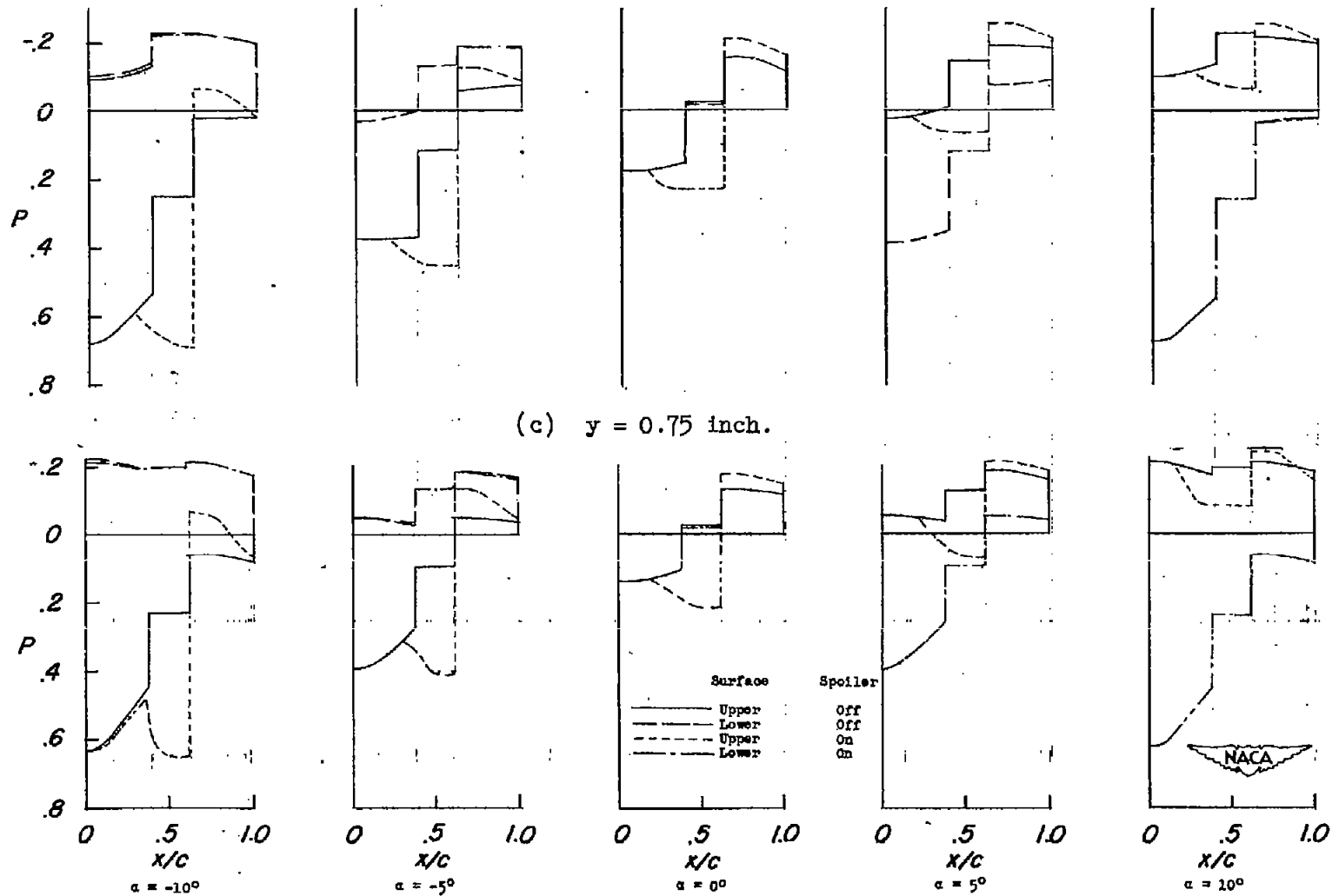
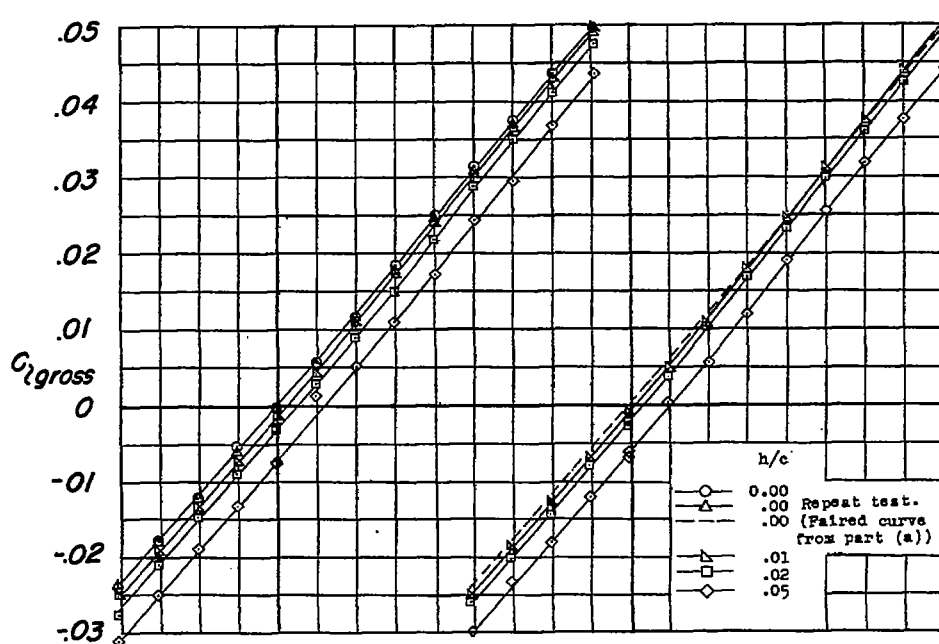
(b)  $y = 2.0$  inches.

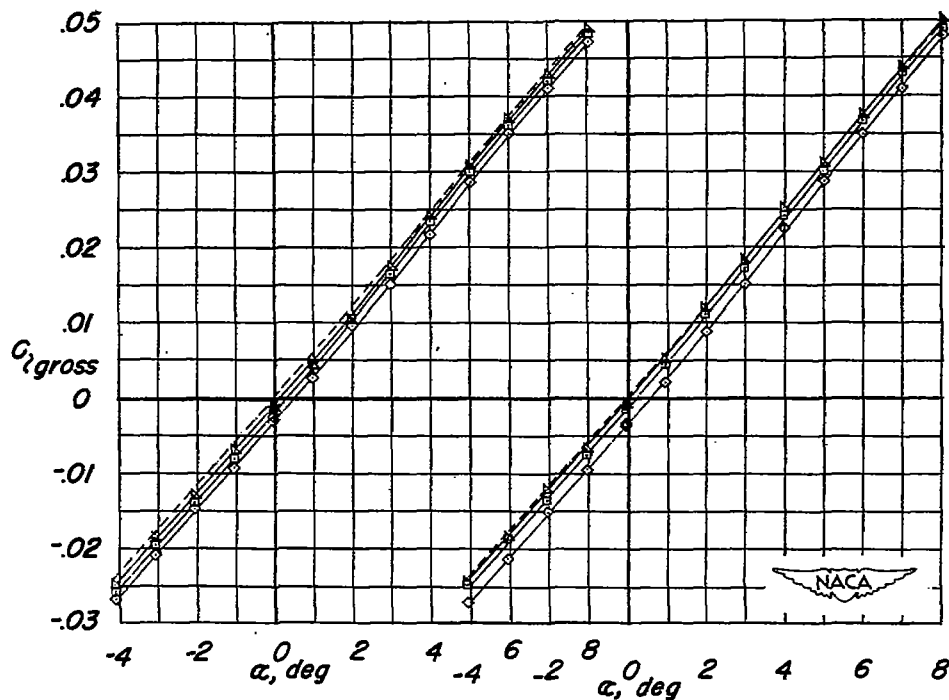
Figure 5.- Calculated and experimental chordwise loading at various spanwise stations from a fuselage of an unswept airfoil with and without a spoiler projected  $0.05c$  and located at  $0.62c$  station.  $M = 1.96$ ;  
 $R = 1.3 \times 10^6$ .





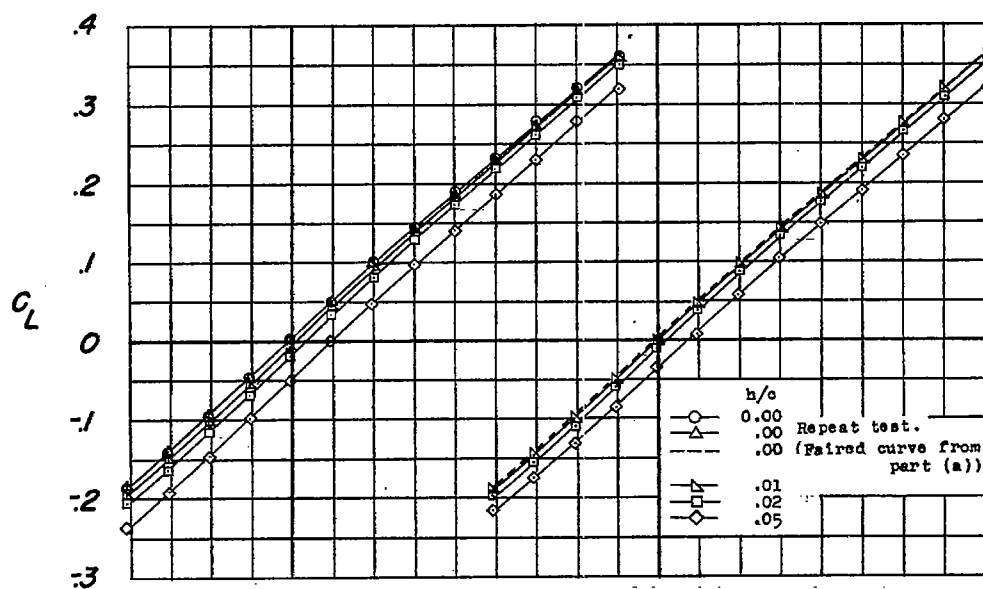


(a)  $b_s = 0.75b/2$ ,  $y_s = 0.20b/2$ . (b)  $b_s = 0.50b/2$ ,  $y_s = 0.45b/2$ .

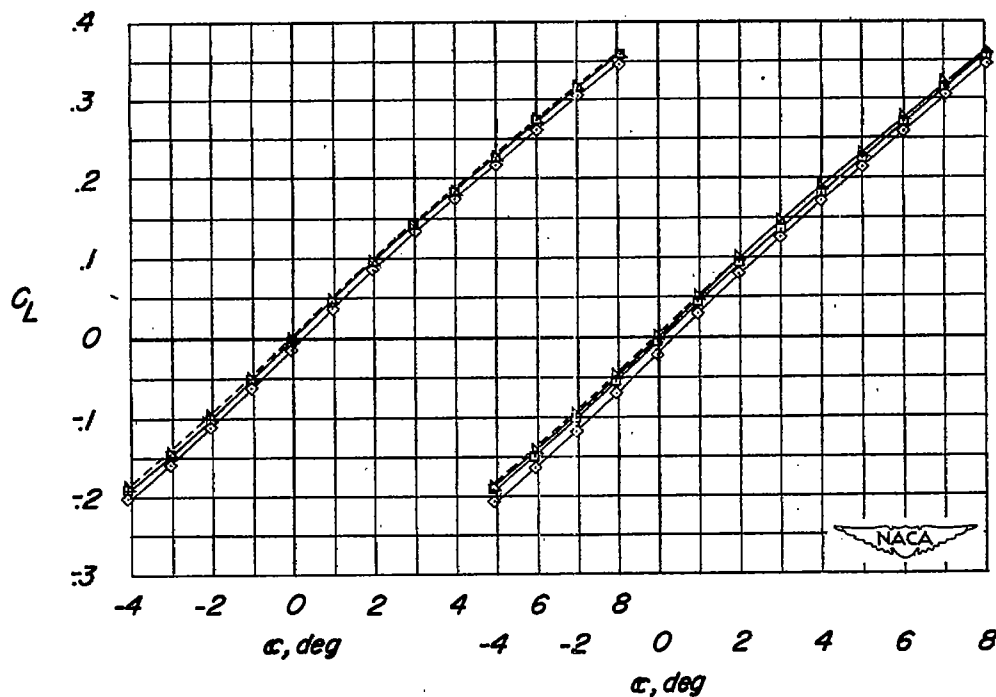


(c)  $b_s = 0.25b/2$ ,  $y_s = 0.70b/2$ . (d)  $b_s = 0.25b/2$ ,  $y_s = 0.45b/2$ .

Figure 6.- Rolling-moment characteristics of an unswept semispan wing with spoilers located at the  $0.75c$  station.  $R = 2.2 \times 10^6$ ;  $M = 1.90$ .

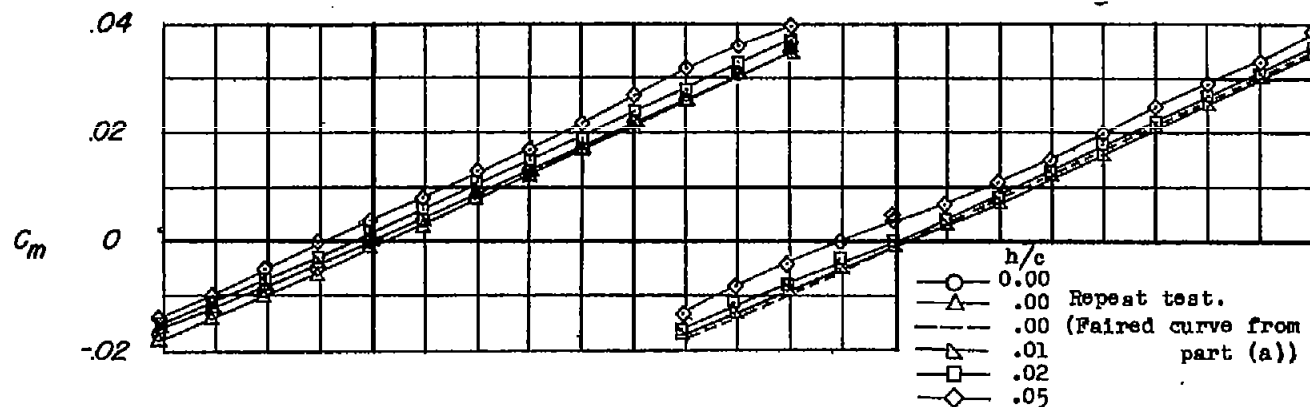


(a)  $b_s = 0.75b/2$ ,  $y_s = 0.20b/2$ . (b)  $b_s = 0.50b/2$ ,  $y_s = 0.45b/2$ .

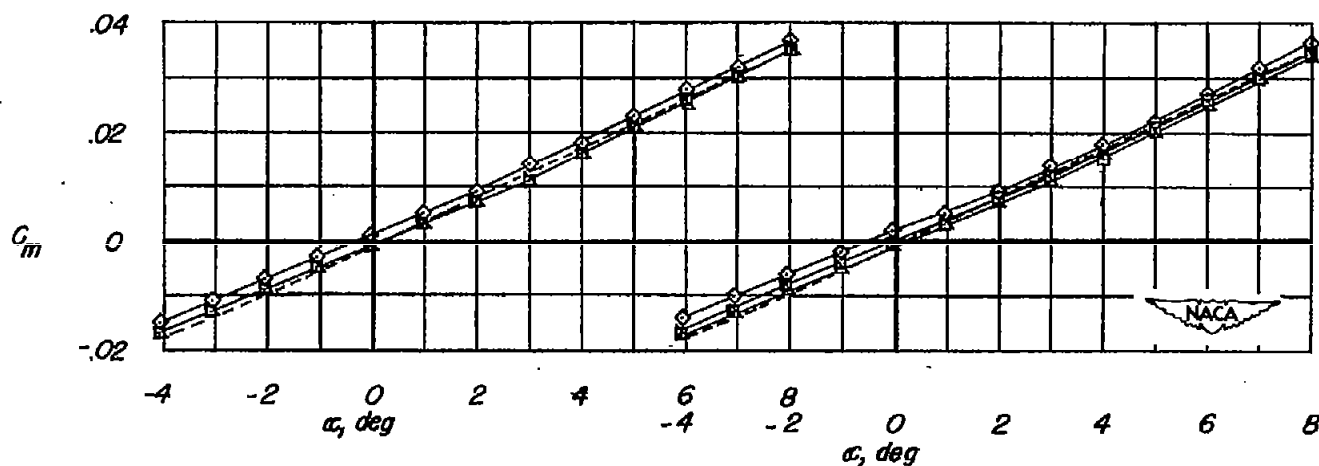


(c)  $b_s = 0.25b/2$ ,  $y_s = 0.70b/2$ . (d)  $b_s = 0.25b/2$ ,  $y_s = 0.45b/2$ .

Figure 7.- Lift characteristics of an unswept semispan wing with spoilers located at the  $0.75c$  station.  $R = 2.2 \times 10^6$ ;  $M = 1.90$ .



(a)  $b_s = 0.75b/2$ ,  $y_s = 0.20b/2$ . (b)  $b_s = 0.50b/2$ ,  $y_s = 0.45b/2$ .



(c)  $b_s = 0.25b/2$ ,  $y_s = 0.70b/2$ . (d)  $b_s = 0.25b/2$ ,  $y_s = 0.45b/2$ .

Figure 8.- Pitching-moment characteristics of an unswept semispan wing with spoilers located at the  $0.75c$  station.  $R = 2.2 \times 10^6$ ;  $M = 1.90$ .

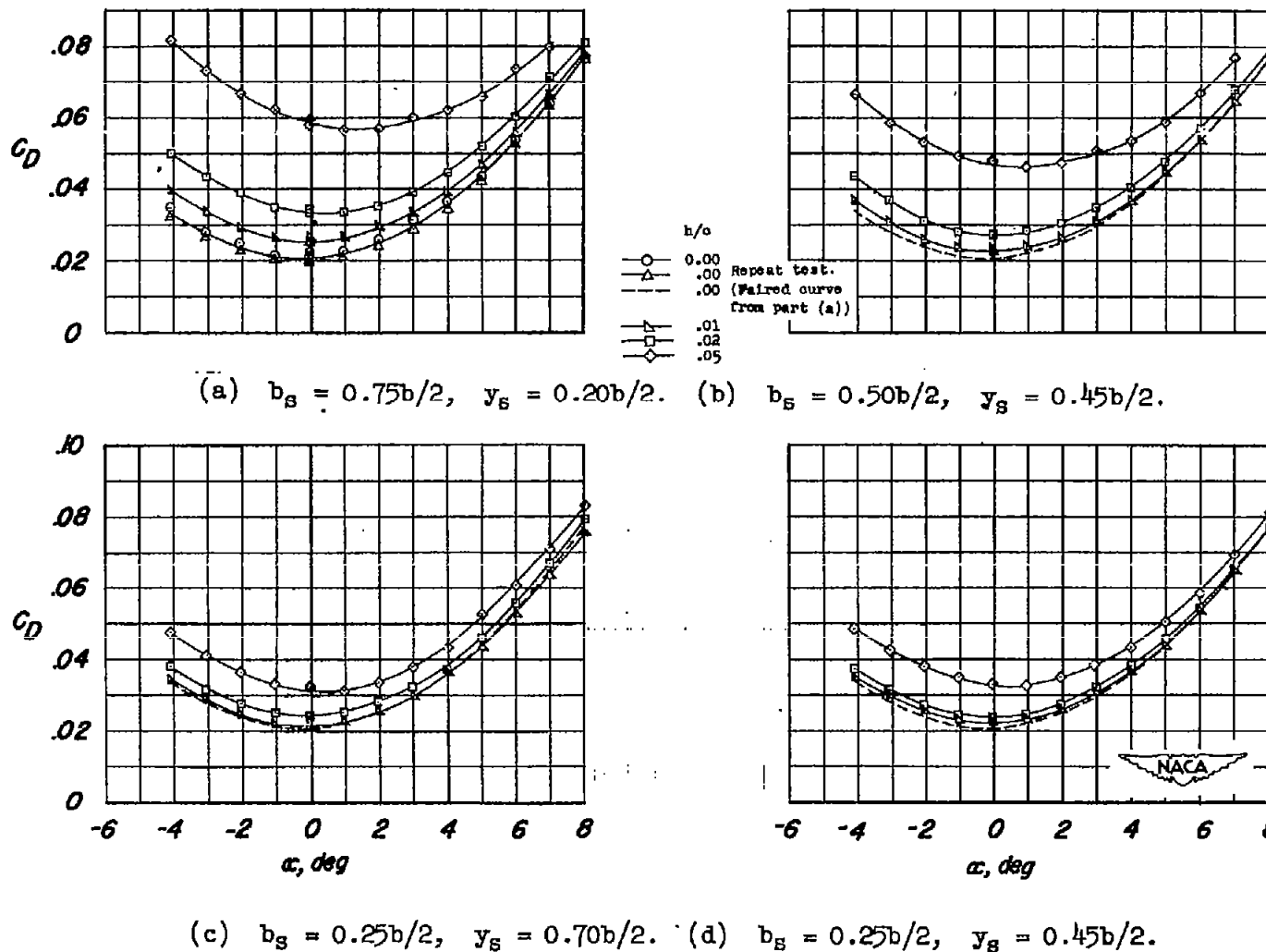


Figure 9.- Drag characteristics of an unswept semispan wing with spoilers located at the  $0.75c$  station.  $R = 2.2 \times 10^6$ ;  $M = 1.90$ .

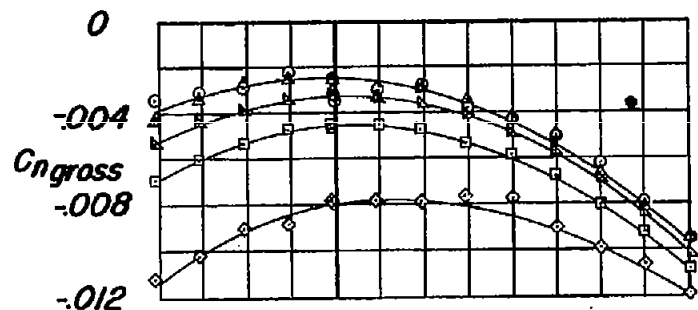
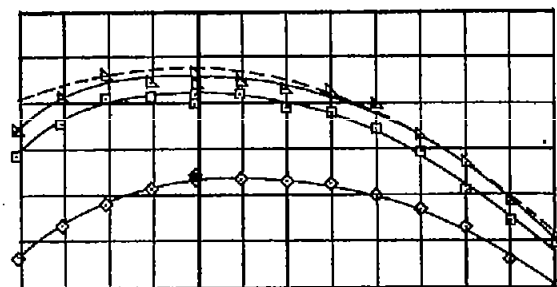
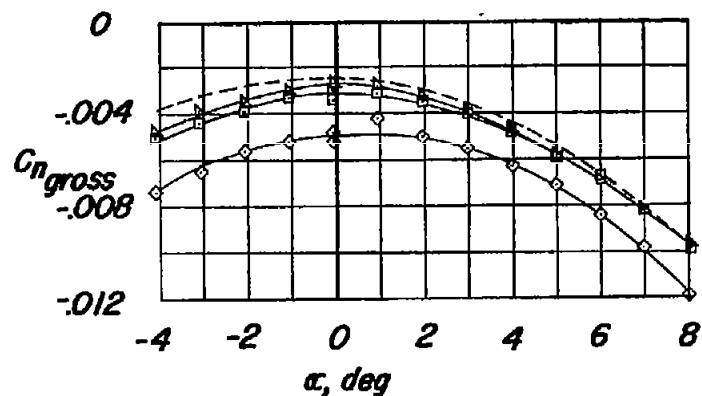
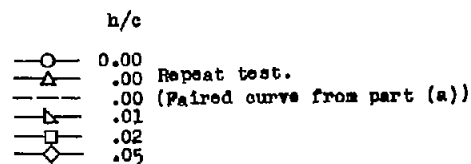
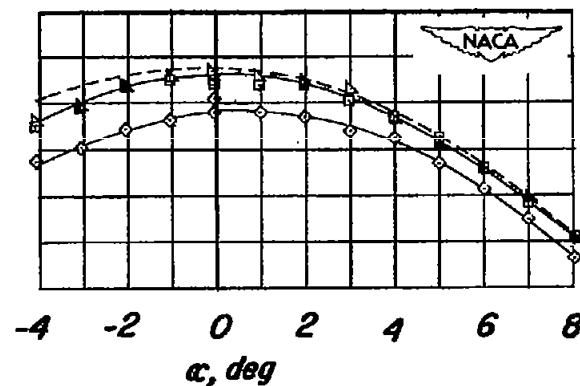
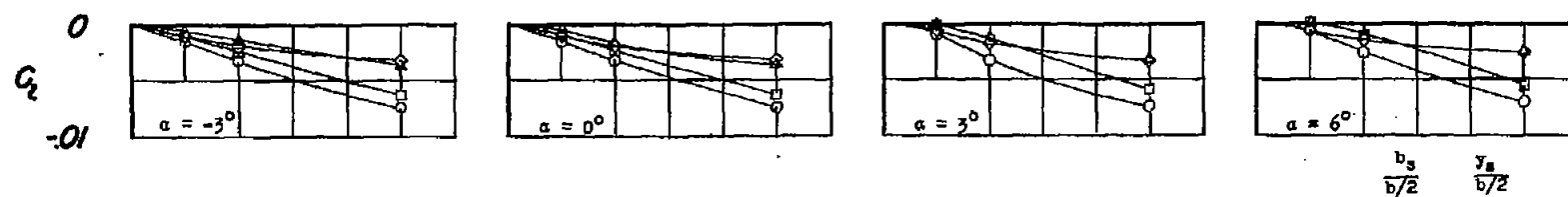
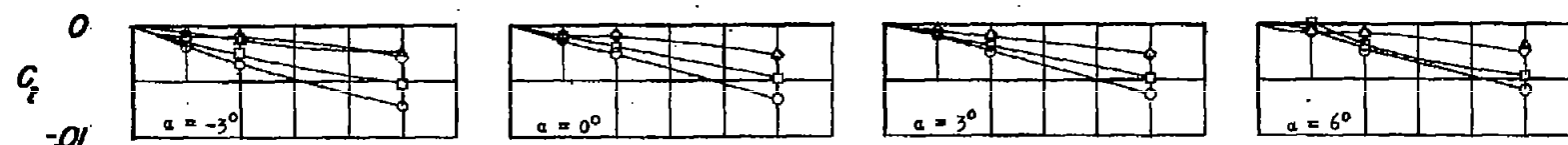
(a)  $b_s = 0.75b/2$ ,  $y_s = 0.20b/2$ .(b)  $b_s = 0.50b/2$ ,  $y_s = 0.45b/2$ .(c)  $b_s = 0.25b/2$ ,  $y_s = 0.70b/2$ .(d)  $b_s = 0.25b/2$ ,  $y_s = 0.45b/2$ .

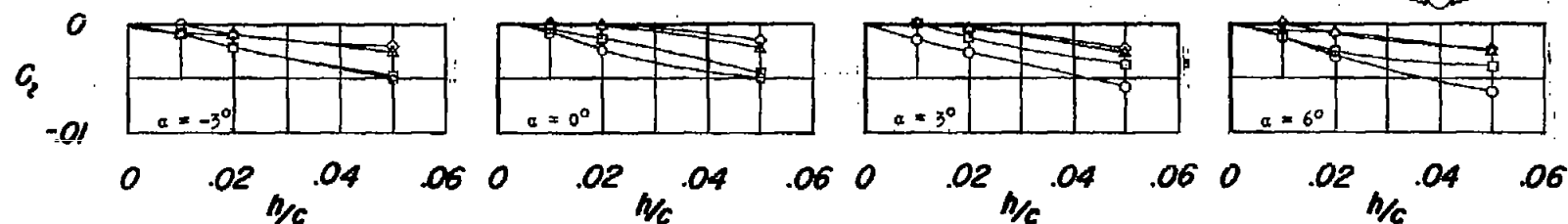
Figure 10.- Yawing-moment characteristics of an unswept semispan wing with spoilers located at the  $0.75c$  station.  $R = 2.2 \times 10^6$ ;  $M = 1.90$ .



(a) Spoilers located at the 0.75c station.

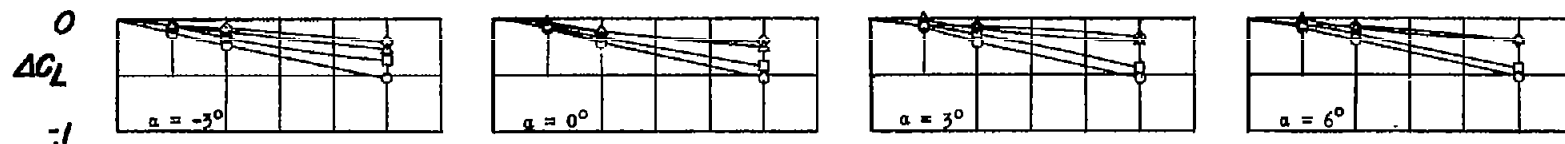


(b) Spoilers located at the 0.65c station.



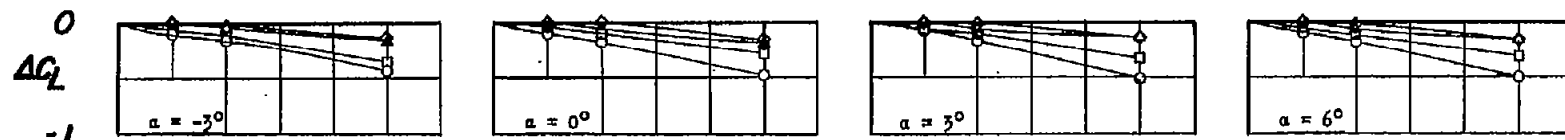
(c) Spoilers located at the 0.55c station.

Figure 11.- Rolling-moment characteristics of an unswept semispan wing equipped with spoiler-type controls.  $R = 2.2 \times 10^6$ ;  $M = 1.90$ .

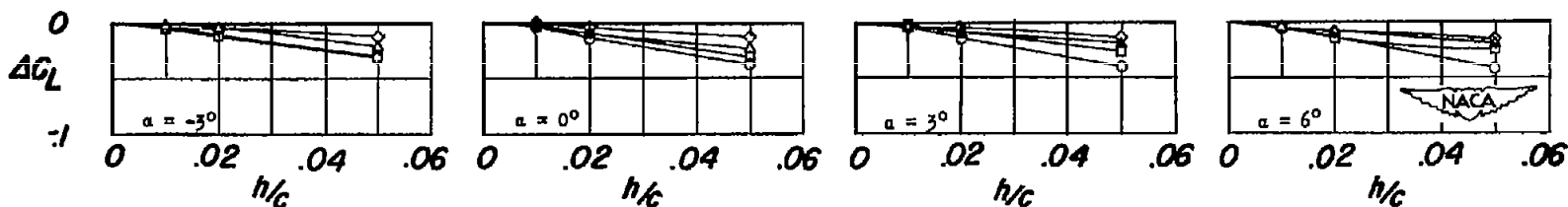


	$\frac{b_s}{b/2}$	$\frac{y_s}{b/2}$
○	0.75	0.20
□	.50	.45
◇	.25	.70
Δ	.25	.45

(a) Spoilers located at the 0.75c station.



(b) Spoilers located at the 0.65c station.



(c) Spoilers located at the 0.55c station.

Figure 12.- Lift characteristics of an unswept semispan wing equipped with spoiler-type controls.  $R = 2.2 \times 10^6$ ;  $M = 1.90$ .

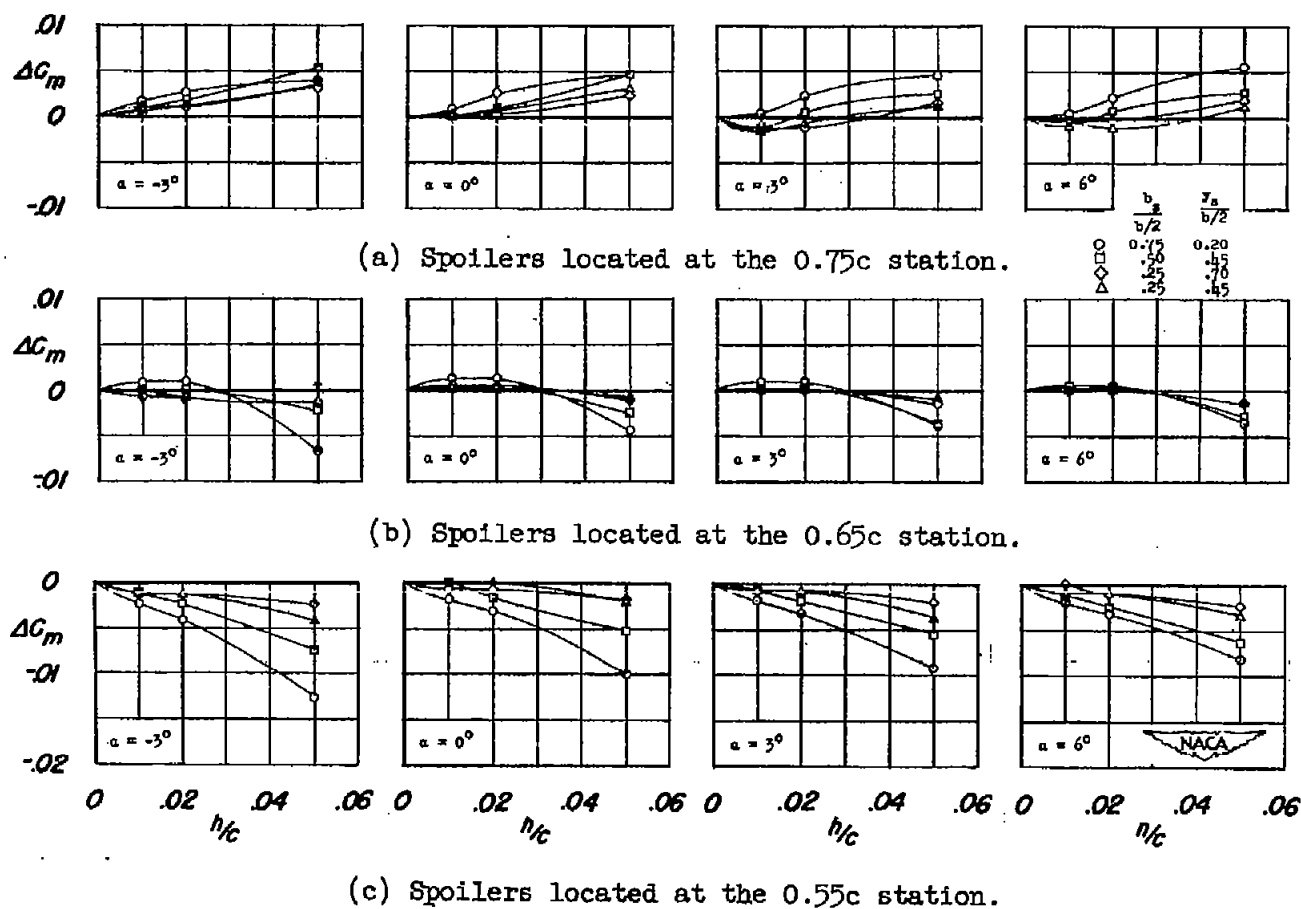
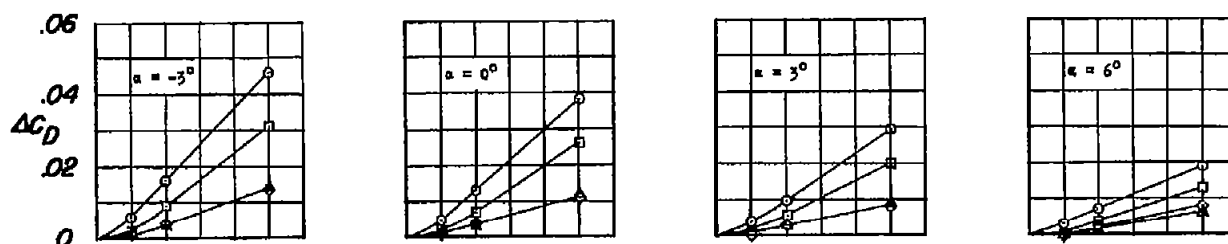
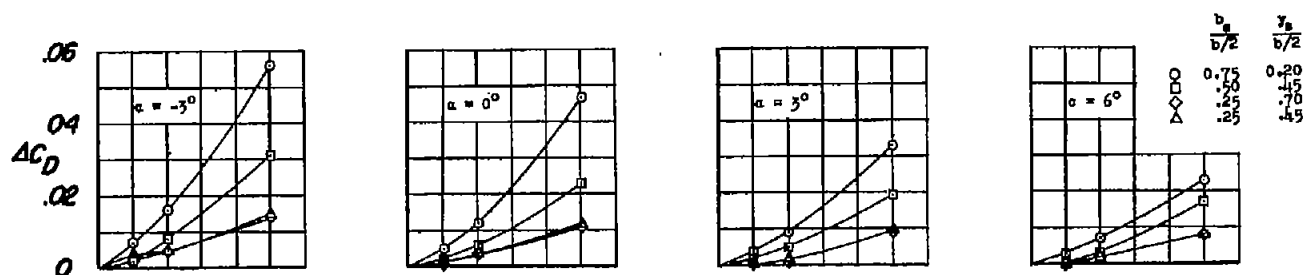


Figure 13.- Pitching-moment characteristics of an unswept wing equipped with spoiler-type controls.  $R = 2.2 \times 10^6$ ;  $M = 1.90$ .

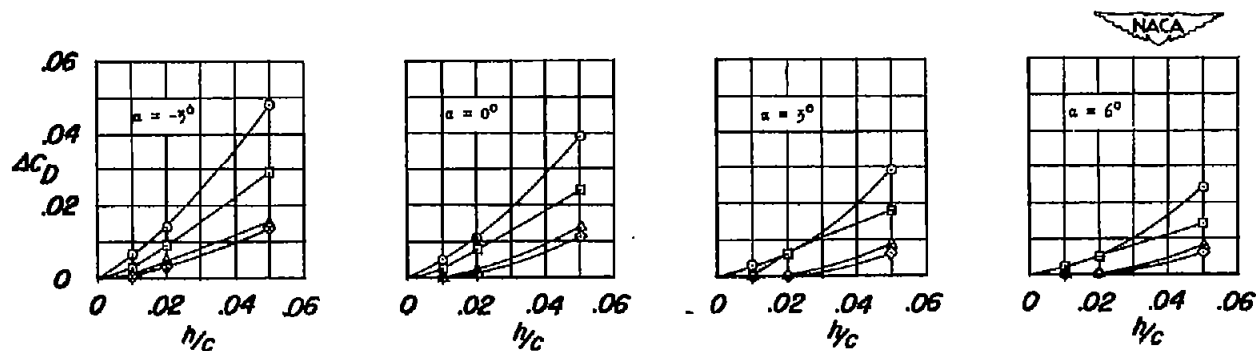




(a) Spoilers located at the 0.75c station.

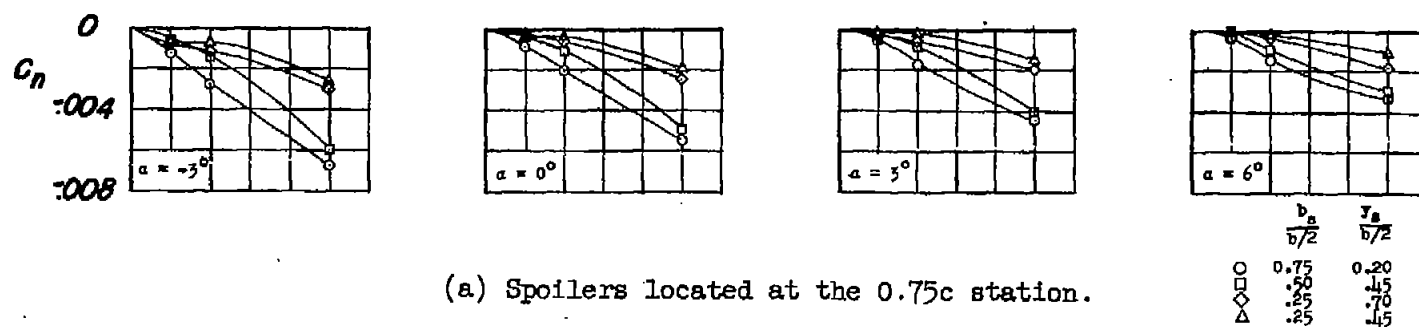


(b) Spoilers located at the 0.65c station.

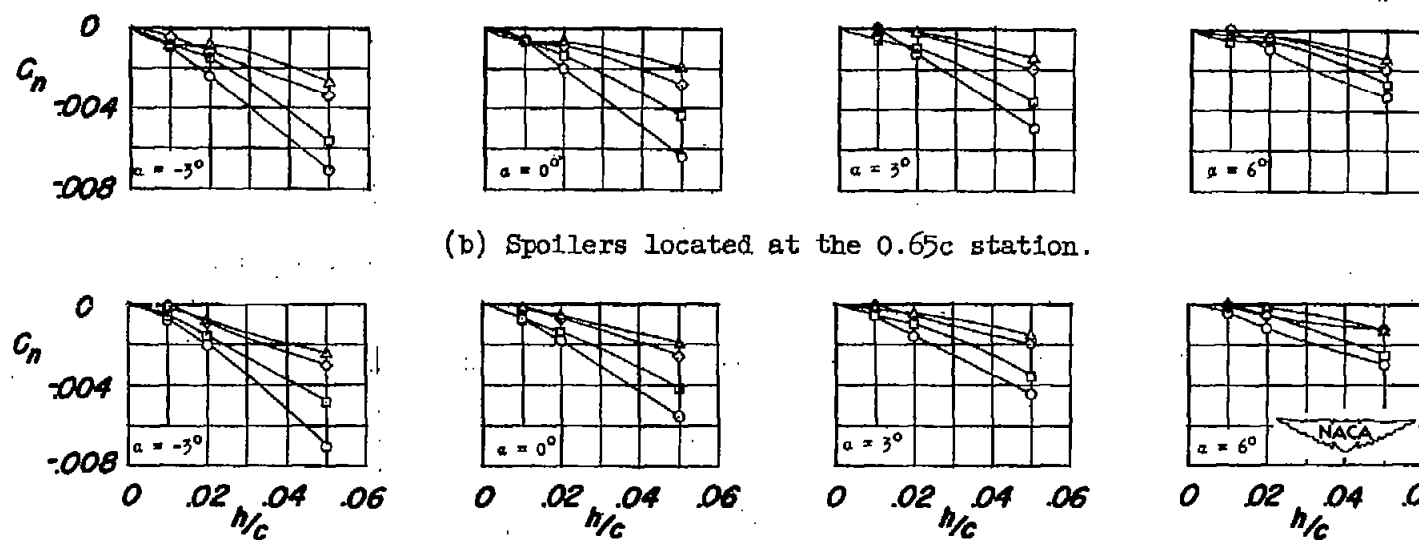


(c) Spoilers located at the 0.55c station.

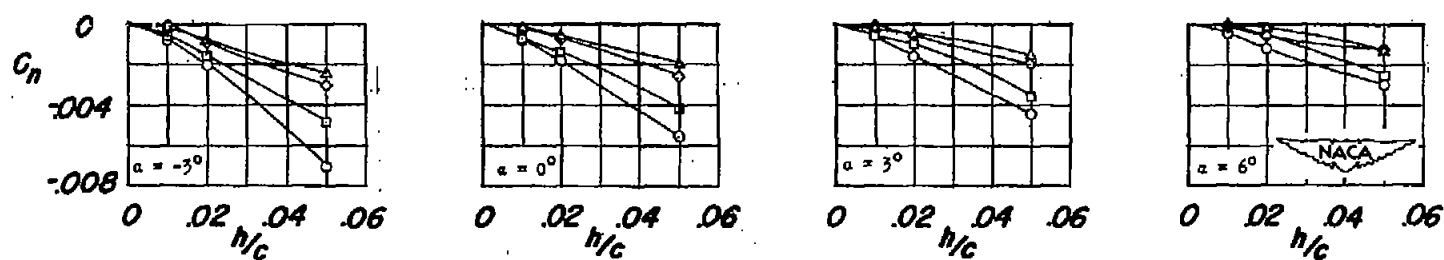
Figure 14.- Drag characteristics of an unswept semispan wing equipped with spoiler-type controls.  $R = 2.2 \times 10^6$ ;  $M = 1.90$ .



(a) Spoilers located at the 0.75c station.



(b) Spoilers located at the 0.65c station.



(c) Spoilers located at the 0.55c station.

Figure 15.-- Yawing-moment characteristics of an unswept semispan wing equipped with spoiler-type controls.  $R = 2.2 \times 10^6$ ;  $M = 1.90$ .

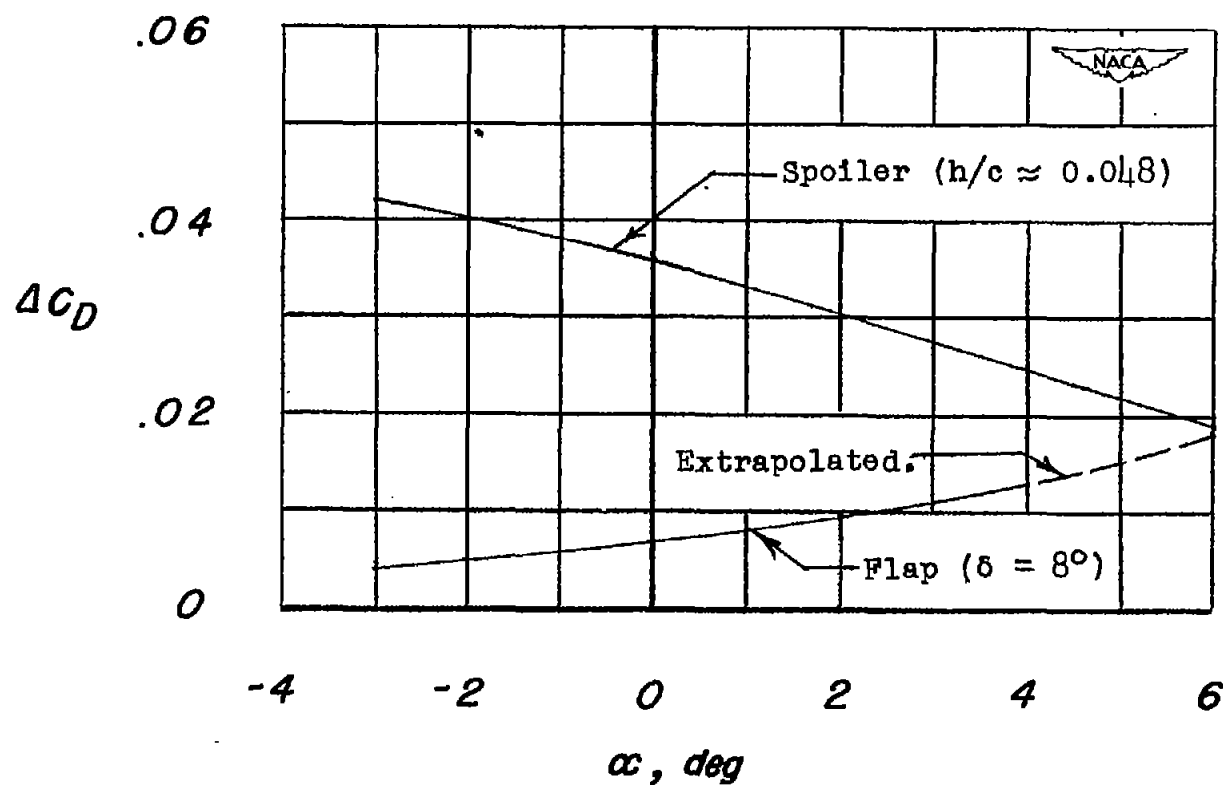


Figure 16.- Variation with angle of attack of drag increment attributed to spoiler-type or flap-type aileron deflected to produce  $C_l = 0.007$ . Aileron span =  $0.75b/2$ ; aileron chordwise location =  $0.75c$ ; spoiler deflected from upper surface; flap trailing edge deflected down;  $M = 1.90$ ;  $R = 2.2 \times 10^6$ .